Science of the Total Environment 514 (2015) 439–449

Contents lists available at ScienceDirect

Science of the Total Environment

journal homepage: www.elsevier.com/locate/scitotenv

A multi-scale health impact assessment of air pollution over the 21st century

Victoria N. Likhvar [a,*], Mathilde Pascal [b], Konstantinos Markakis [c], Augustin Colette [d], Didier Hauglustaine [e], Myrto Valari [f], Zbigniew Klimont [g], Sylvia Medina [h], Patrick Kinney [i]

[a] LSCE, Laboratoire des Sciences du Climat et de l'Environnement, CEN Saclay-Orme des Merisiers-Bat. 712, F-91191 Gif-sur-Yvette CEDEX, France
[b] InVS, French Institut of Public Health Surveillance (Institut de Veille Sanitaire), 12 rue du Val-d'Osne, 94415 Saint-Maurice Cédex, France
[c] LMD, Laboratoire de Météorologie Dynamique, IPSL Laboratoire CEA/CNRS/UVSQ, Ecole Polytechnique, 91128 Palaiseau Cedex, France
[d] INERIS, Institut National de l'Environnement Industriel et des Risques, BP2 60550 Verneuil-en-Halatte, France
[e] LSCE, Laboratoire des Sciences du Climat et de l'Environnement, CEN Saclay-Orme des Merisiers-Bat. 712, F-91191 Gif-sur-Yvette CEDEX, France
[f] LMD, Laboratoire de Météorologie Dynamique, IPSL Laboratoire CEA/CNRS/UVSQ, Ecole Polytechnique, 91128 Palaiseau Cedex, France
[g] IIASA, International Institute for Applied Systems Analysis, Schlossplatz 1, 2361 Laxenburg, Austria
[h] InVS, French Institut of Public Health Surveillance (Institut de Veille Sanitaire), 12 rue du Val-d'Osne, 94415 Saint-Maurice Cédex, France
[i] Columbia University in the City of New York, 722 West 168th Street, Room 1104E, New York, NY 10032, United States

HIGHLIGHTS

- We assessed impact of air pollution on health in 2030–2050.
- We used two ECLIPSE emissions scenarios (CLE, MFR) on three geographical scales.
- We projected larger impacts on CV and respiratory mortality under the MFR scenario.
- The impacts can be larger on finer scale, due to a resolution or a model choice.
- Multi-scale HIA can provide relevant results for decision-makers.

ARTICLE INFO

Article history:
Received 2 December 2014
Received in revised form 17 January 2015
Accepted 1 February 2015
Available online xxxx

Editor: Xuexi Tie

Keywords:
Health impact assessment
Air quality modeling
Emissions scenarios
Cardiovascular disease
Particulate matter

ABSTRACT

Background: Ozone and $PM_{2.5}$ are current risk factors for premature death all over the globe. In coming decades, substantial improvements in public health may be achieved by reducing air pollution. To better understand the potential of emissions policies, studies are needed that assess possible future health impacts under alternative assumptions about future emissions and climate across multiple spatial scales.
Method: We used consistent climate–air-quality–health modeling framework across three geographical scales (World, Europe and Ile-de-France) to assess future (2030–2050) health impacts of ozone and $PM_{2.5}$ under two emissions scenarios (Current Legislation Emissions, CLE, and Maximum Feasible Reductions, MFR).
Results: Consistently across the scales, we found more reductions in deaths under MFR scenario compared to CLE. 1.5 [95% CI: 0.4, 2.4] million CV deaths could be delayed each year in 2030 compared to 2010 under MFR scenario, 84% of which would occur in Asia, especially in China. In Europe, the benefits under MFR scenario (219000 CV deaths) are noticeably larger than those under CLE (109000 CV deaths). In Ile-de-France, under MFR more than 2830 annual CV deaths associated with $PM_{2.5}$ changes could be delayed in 2050 compared to 2010. In Paris, ozone-related respiratory mortality should increase under both scenarios.
Conclusion: Multi-scale HIAs can illustrate the difference in direct consequences of costly mitigation policies and provide results that may help decision-makers choose between different policy alternatives at different scales.

1. Introduction

Numerous epidemiological studies have shown that exposure to outdoor air pollution (OAP) leads to adverse health outcomes, including increases in mortality and morbidity for cardiovascular and respiratory diseases (Beelen et al., 2013; Hoek et al., 2013; Krewski et al., 2009; Pope et al., 2002; Pope and Dockery, 2006; Raaschou-Nielsen et al.,

* Corresponding author.
E-mail addresses: vlikhvar@gmail.com (V.N. Likhvar), m.pascal@invs.sante.fr (M. Pascal), konstantinos.markakis@lmd.polytechnique.fr (K. Markakis), augustin.colette@ineris.fr (A. Colette), didier.hauglustaine@lsce.ipsl.fr (D. Hauglustaine), myrto.valari@lmd.polytechnique.fr (M. Valari), klimont@iiasa.ac.at (Z. Klimont), s.medina@invs.sante.fr (S. Medina), plk3@columbia.edu (P. Kinney).

http://dx.doi.org/10.1016/j.scitotenv.2015.02.002
0048-9697/

2013). The International Agency for Research on Cancer (IARC) recently classified OAP (including particulate matter (PM) as a major component of it) as carcinogenic to humans (Group 1) (IARC, 2013). While individual-level health risks associated with OAP may be low compared to other risk factors, the overall population-wide public-health impact can be very large. For instance, according to the World Health Organization's Global Burden of Diseases (Lozano et al., 2012), in 2010, annually, 3.22 million people died prematurely because of outdoor PM, and 0.15 million because of ozone (O_3).

Health impact assessments (HIAs) have been extensively used to quantify the public-health impact of OAP and to help decision-makers understand the benefits that would be associated with an improved air quality (Medina et al., 2013). With the development of air quality and climate models, there is a growing interest in quantifying the future health-impacts of air pollution, taking into account trends in emissions, air-pollution policies and climate change. Joint policies to reduce emissions of air pollutants and greenhouse gases are promising, as climate and air pollutants are associated through dynamic processes at multiple scales, from common emission sources to their chemical and physical interactions in the atmosphere (Colette et al., 2012b; Jacob and Winner, 2009). HIA can help in understanding the health benefits that could potentially be achieved under different scenarios of air pollution emissions and of climate change, and therefore encourage synergies and limit trade-offs between mitigation of climate change and mitigation of air pollution.

Several HIAs examining future air pollution-related health impacts have been published using a range of climate and air quality models, scenarios, and spatial/temporal scales (Anenberg et al., 2012; Heal et al. 2012; Post et al., 2012; Orru et al., 2013). The choice of appropriate spatial and temporal scale to make such exercise meaningful to decision-makers is a crucial issue. In this paper, we present and compare HIAs of future air pollution carried out in a consistent way across three different geographical scales: the World, Europe and the French Ile-de-France (IdF) region. Our focus here is on health impacts rather than on modeling issues. The objective is two-fold: for scientists, it allows comparing the results across scales; for decision-makers, it allows putting the results into a large perspective illustrating that air quality and climate change are not only global, but also local issues.

2. Materials and methods

2.1. General framework and scenarios

To quantify the health impacts of OAP on three geographical scales we used alternative scenarios for air pollutant emissions, and climate change (Fig. 1). These emissions scenarios were inputs to climate and chemistry models, which were coupled across the scales.

We used two air pollution emissions scenarios consistent across the scales, the "Current Legislation Emissions" (CLE) and the "Maximum Feasible Reduction" (MFR). These scenarios were developed in the framework of the ECLIPSE (Evaluating the Climate and Air Quality Impacts of Short-Lived Pollutants) project (Amman et al., 2013; Klimont et al., 2013, in preparation for ACPD). They include both climate and regional air quality policies for the emissions of air pollutants. The CLE scenario assumes that the existing air quality legislation is fully implemented and enforced. The MFR assumes that all technologically feasible emission reduction measures are implemented. It is computed using the lowest range of emission factors in the GAINS (Greenhouse Gas and Air Pollution Interactions and Synergies) model (Amann et al., 2011) but ignores any non-technical measures. It has to be noted that while indeed the air quality policies should be mostly enforced until 2030 (Amman et al., 2013) there still might be significant changes, that is, in some world regions the activity data (e.g., economic growth) might lead to strong increases in air pollution and rebound air pollution effects unless stronger legislation is introduced. The CO_2 trajectory of ECLIPSE is similar (at a global level) to the RCP6.0 but the emission of pollutants develops differently, typically the RCPs reduce emissions much quicker than CLE in ECLIPSE/GAINS and the reasons of that were discussed in Amman et al. (2013).

From the ECLIPSE database we used anthropogenic emissions. We used Lathière et al. (2006) for biogenic emissions, Koffi et al. (2010) for the aviation and shipping emissions, and van der Werf et al. (2010) for forest and savannah burning emissions. Other source emissions were calculated within the air pollution models. For each scale, we performed two sets of continuous simulations, one for the present time and another one for the two future ECLIPSE-V4a projections. The air pollutant emissions used for the three time frames are those of 2010, 2030 and 2050 and for the sake of simplification we will use these labels in the following sections of the paper.

2.2. Climate modeling

At the global scale, we used meteorological data from the European Center for Medium-Range Weather Forecasts (ECMWF) reanalysis. To isolate the impact of anthropogenic emissions, we performed simulations under the present-day climate conditions (2005–2006). The impact of future climate change on particles and chemistry was not taken into account; we used the results of the 2006 meteorological conditions in all simulations. The role played by climate change and

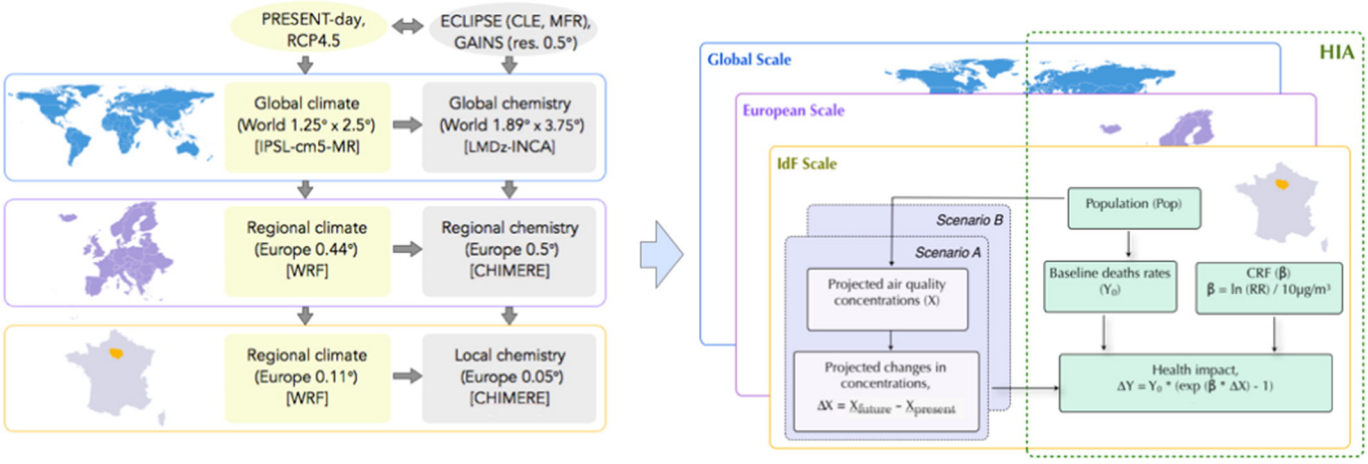

Fig. 1. The scheme of air pollution and climate modeling (left) and HIA method (right) framework: at each scale a climate model feeds a chemistry model to assess future concentrations of air pollutants, which are used in the HIA analysis. In the round brackets: (geographical area of the modeling and the size of the grid cells). In the square brackets: [name of the model].

the impact of nitrate on the indirect aerosol radiative forcing of climate will be investigated in a forthcoming study.

At the European scale, the future evolution of climate was assessed using the IPSL-cm5-MR member of CMIP5 global-scale model (Taylor et al., 2012) downscaled spatially at a resolution of 0.44° with the WRF meteorological model (Skamarock et al., 2008) used as regional climate model. The simulations used are the low-resolution IPSL-INERIS member of the Euro-Cordex ensemble (Jacob et al., 2013). The RCP4.5 radiative forcing pathway was used to drive the climate simulations.

The meteorology for IdF derived from the high-resolution IPSL-INERIS member of the Euro-Cordex ensemble of regional climate model simulations at 0.11° (~10 km) resolution over Europe.

2.3. Air pollution modeling

2.3.1. Global scale

The future evolution of global atmospheric composition has been simulated with the LMDz-INCA global chemistry–aerosol–climate model coupling on-line the LMDz (Laboratoire de Météorologie Dynamique, version 5) General Circulation Model (GCM) (Hourdin et al., 2006) and the INCA (INteraction with Chemistry and Aerosols, version 4) model (Hauglustaine et al., 2004). In the present configuration, the model includes 39 hybrid vertical levels. The horizontal resolution is 1.89° in latitude and 3.75° in longitude, which is equivalent to 201 km in the mid-latitude. For a more detailed description and an extended evaluation of the GCM we refer to Hourdin et al. (2006). INCA includes a state-of-the-art CH4-NOx-CO-NMHC-O_3 tropospheric photochemistry (Hauglustaine et al., 2004; Folberth et al., 2006). The tropospheric photochemistry and aerosol scheme used in this model version are described through a total of 123 tracers including 22 tracers to represent aerosols. For aerosols, the INCA model simulates the distribution of aerosols with anthropogenic sources such as sulfates, nitrates, black carbon, particulate organic matter, as well as natural aerosols such as sea-salt and dust (Schulz, 2007; Balkanski, 2011; Hauglustaine et al., 2014).

2.3.2. European scale

To model the impact of future emissions on air pollution concentrations in Europe at a regional scale, we used the CHIMERE chemical transport model (Menut et al., 2013) that computes the fate of primary and secondary pollutants (including secondary inorganic and organic aerosols). The model has been widely used for research applications involving historical air quality (Bessagnet et al., 2004, 2008; Vautard et al., 2005) as well as operational air quality forecasting (Rouïl et al., 2009; Zhang et al., 2012). It has been benchmarked in terms of O_3 and PM to other existing tools in various model inter-comparison exercises (van Loon et al., 2007; Vautard et al., 2009), some of which focused on long term simulations (Colette et al., 2011, 2012a). We used the model outputs at 0.5° (~50 km) resolution covering Europe.

The chemical boundary conditions were obtained from a 10-year average of chemical composition over Europe simulated with the global LMDz-INCA model for the present day (Szopa et al., 2012).

2.3.3. Ile-de-France scale

The IdF region is located at 1.25°–3.58° east and 47.89°–49.45° north with a population of approximately 11.7 million, more than two million of which live in the city of Paris. The area is situated away from the coast and is characterized by uniform and low topography, not exceeding 200 m above the sea level. To model the air quality in the IdF region we used the CHIMERE model at 0.05° (~4 km) horizontal resolution in a 156 × 128 km domain covering IdF.

Air pollution emissions for IdF were available at hourly intervals with a spatial resolution of 1 × 1 km (aggregated to 4 km). The emissions dataset was compiled by local experts using a variety of city-specific information integrating a number of anthropogenic activities in the region (AIRPARIF, 2012). The spatial allocation of emissions was completed using proxies such as high-resolution population maps, road network and the location of industrial units. Boundary and initial conditions for the IdF simulations were taken from the European scale simulation.

In order to maintain consistency and to be able to compare the results among the scales we harmonized the local inventory in terms of annual emission fluxes with the ECLIPSE estimates used in the regional model. To achieve our goal we synchronize the emission totals of the ECLIPSE and AIRPARIF inventories. We develop a new version of the AIRPARIF inventory by scaling its total annual per pollutant emissions to match the ECLIPSE annual quantified fluxes. The spatial representation and temporal patterns (monthly, weekly, diurnal) of the final inventory are therefore adopted by AIRPARIF. To provide future estimates of emissions in IdF under the CLE and MFR scenarios we employed an equivalent procedure.

2.4. Population and health data

We used gridded world population data, country boundaries and coastlines from the Center for International Earth Science Information Network (CIESIN)/Columbia University, and Centro Internacional de Agricultura Tropical (CIAT) (2005). To avoid discrepancy between the gridded population estimates and the population counts from the WHO mortality database (2011), we adjusted the gridded population data to the population older than 15 for the year 2008. The population counts by commune in IdF were obtained for the year 2009 from the Institut national de la statistique et des études économiques (INSEE).

For the global scale, we obtained the baseline mortality data for 193 countries for 2008 from the WHO mortality database (2011). It gathers mortality data reported annually by Member States from their civil registration systems. The extracted data contain yearly country-specific estimates as number of deaths, death rates and age-standardized death rates for two age-groups (15-59 and older than 60) and are stratified by cause of death: "all-cause" (ICD10); cardiovascular (ICD10: I00-I99); respiratory (ICD10: J30-J98). The European baseline data are obtained from the same set as global data.

For IdF, the mortality data for cardiovascular and respiratory diseases for 1300 communes, for years 2000–2010, were obtained from the CepiDC (France).

Initially, for 2030 and 2050, we kept the baseline mortality data and population data constant. In sensitivity analysis we examined the projected changes in baseline mortality rates and population for 2030 in several world regions, using WHO projections (Mathers and Loncar, 2006).

2.5. HIA method

HIA computes the changes in health outcomes related to changes in air-pollutant concentrations using a concentration–response function (CRF) derived from epidemiological studies. The changes in mortality are estimated using the following equation:

$$\Delta Y = Y_0 * (1 - \exp(-\beta * \Delta X)),$$

where ΔY is the change in incidence rate of the health effect in a given population in the future relative to present, Y_0 is the baseline mortality for a given population, β is the CRF that describes the relationship between a change in the pollutant concentration and the corresponding change in the outcome of the health effect, and ΔX is a change in the air-pollutant concentration.

Considering the current evidence on the health impacts of OAP and health data availability, we decided to focus on the long-term impacts of $PM_{2.5}$ and cardiovascular mortality, and of O_3 on respiratory mortality. For PM, we used the CRF provided by a recent meta-analysis (Hoek et al., 2013). For ozone, we used the relative risk of respiratory disease,

1.040 [95% CI: 1.010, 1.067] per 20 μg/m^3 increase in the summer season average of 1-hour maximum ozone converted to the RR value per 10 μg/m^3 increase in the maximum daily 8-hour ozone mean of the summer season using an 8-hour/1-hour ratio of 0.88 from Jerrett et al. (2009).

We computed ΔX as the difference between the concentrations observed for the future under a given scenario and the 2010 period concentrations.

To produce gridded maps we calculated HIA using projected air pollution for each cell (1° × 1° resolution at the global scale, 4 km × 4 km at the European scale, and 0.4 km × 0.4 km at the IdF scale). For presentation purposes, we aggregated the results into the region, country or department levels using population-weighted air pollution calculated separately for each region of interest at all scales. The countries and regions were chosen according to the WHO classification. Gridded results are presented in the maps and can be requested from the authors.

3. Results

3.1. Particulate matter and ozone concentrations

3.1.1. Global scale

Global $PM_{2.5}$ concentrations for 2010, 2030 and 2050 under two emissions scenarios are shown in Fig. S1. For 2010, the population-weighted global average annual $PM_{2.5}$ concentrations across the countries were estimated at 4.0 (min = 0.3, max = 22.6) μg/m^3. This value is lower than the measured concentrations in several locations but owing to the spatial scale of the global analysis it is considered representative and comparable to other assessments (Rao et al., 2013). In 2030, this level would decrease by about 0.2 μg/m^3 under CLE and by 1.9 μg/m^3 under MFR. The future changes exhibit considerable geographic heterogeneity, as illustrated in Supplemental Fig. S2 for six world regions.

Future concentrations under CLE scenario are very similar to the present situation (it is not necessarily when the analysis is done at a finer spatial resolution, such as European and IdF; see Sections 3.1.2 and 3.1.3), compared to MFR, under which large reductions are projected. A large part of the population will remain exposed to concentrations above the WHO guideline values (10 μg/m^3 for $PM_{2.5}$). The 34% of the world population could be exposed to $PM_{2.5}$ >10 μg/m^3 in 2010. In 2030, it could be 42% under CLE and 1% under MFR. These numbers would worsen giving the fact that many countries have their own standards that tend to be stricter than WHO's.

In Asia, the $PM_{2.5}$ could increase by 18% under CLE scenario in 2050. Under the more aggressive emissions reduction scenario represented by the MFR, the average concentrations could decrease in Asia by 57% by 2030, especially in China (77% decrease).

Similarly large percentage reductions are projected for Europe and northern America in 2030 under MFR; the PM concentrations could decrease by 63% and 56%, respectively. In Latin America the concentrations could decrease by 32% under MFR. Similar results were estimated for Sub-Saharan (SS) Africa, where the largest improvements were projected in the southern regions (52% decrease) and lowest in the central part of SS Africa (13%) by 2030. However, under CLE, in some regions of Latin America (southern and tropical) and SS Africa (central and west) the concentrations are projected to continue to increase.

Global O_3 concentrations for 2010, 2030 and 2050 under two emissions scenarios are shown in Supplementary Fig. S3. For 2010, the population-weighted global average summer O_3 MDA1 concentrations across the countries were estimated at 73 (min = 21, max = 129) μg/m^3. In 2030, these levels would not change under CLE and would decrease by 11 μg/m^3 under MFR. The geographical heterogeneity is also high across the countries. In 2010, the largest O_3 levels are projected in Europe and North America regions (in each of these regions the level was 102 μg/m^3 on average across the countries), which could decrease by 17% and 16% in 2030 relative to 2010 under MFR, respectively. Under CLE, the decreases in Europe and North America in 2030 are 6% and 5%, respectively. In North Africa/Middle East, the 2010 concentrations and changes under both scenarios in 2030 are close to the European and North American changes. In Asia, in 2010, the average O_3 level across the countries was 79 μg/m^3. The future percent changes in O_3 concentrations in Asia in 2030 relative to 2010 are similar to the European changes (17%). By contrast, under CLE, in Asia, North Africa/Middle East and Sub-Saharan Africa, the levels are projected to be larger by 7%, 6% and 2% in 2030 than it was in 2010, respectively.

3.1.2. European scale

Modeled O_3 and $PM_{2.5}$ concentrations in 2010 and 2030 under two emissions scenarios are shown in Fig. S4 (Supplementary material).

Our estimates for 2010 $PM_{2.5}$ matched existing model estimates, with the well-documented hotspots of anthropogenic particulate pollution in the Benelux, South Poland, the Po-Valley (Thunis et al., 2007). The 42% of European population is exposed to the levels of $PM_{2.5}$ larger than 10 μg/m^3. The future evolution of $PM_{2.5}$ exhibits a strong reduction compared to 2010 levels. Under CLE, the main hotspots would remain visible. Under MFR, the PM levels would be significantly reduced.

Similar results as for $PM_{2.5}$ were obtained for O_3. In 2010, the high O_3 levels are projected over the Mediterranean and neighboring countries. Major pollution hotspots also stand out in Central Europe. Efficient reductions occur over most continental areas by 2050 but high O_3 levels remain over sea surfaces (where increase in sunny days, temperatures and decrease of precipitation are more favorable to ozone build-up and the deposition sink is less efficient). This feature was found in particular over the Mediterranean, to such extent that O_3 levels remain high over Spain, Italy, Greece and Balkan countries. Over Turkey, it is even an O_3 increase that we find by 2030 and 2050 compared to present-day levels (Fig. S4, Supplementary material).

3.1.3. Ile-de-France scale

Modeled O_3 and $PM_{2.5}$ concentrations in 2010 and 2050 under two emissions scenarios are shown in Fig. S5 (Supplementary material).

In IdF, the 2010 population-weighted annual average $PM_{2.5}$ concentration level ranged from 10 to 21 μg/m^3 across the region; the entire population is exposed to levels higher than WHO guideline values. The largest concentrations were projected in the city of Paris (over 20 μg/m^3). Future concentrations are projected to decrease relative to 2010: by 49% under CLE and by 69% under MFR. This is mainly due to the significant reductions in primary particle emissions. The reductions were stronger in the city of Paris than in rural areas due to the effective mitigation of road transport emissions (Markakis et al., 2014).

The 2010 population-weighted summer (June–August) MDA1 O_3 concentrations ranged from 87 to 102 μg/m^3 across the region. Lower O_3 levels (87–91 μg/m^3) over the city of Paris are due to titration by NO (road transport mainly). On average by 2050 the gridded concentrations are projected to decrease by 9% under CLE and by 13% under MFR, mostly in rural areas. In the city area of Paris, we expect increases in concentrations by 4% under CLE and by 2% under MFR, due to reduced NO titration. By contrast, in rural areas the O_3 concentrations will decrease by 8.9% under CLE and by 12.4% under MFR.

3.2. Health impact assessment

There were 17 242 804 of CV deaths recorded in the world, 2 775 396 of which occur in Europe, and 154 741 in France. In 2030, under CLE, the total CV deaths in the world could increase by 6600 (+0.04%) due to the changes in $PM_{2.5}$ concentrations. Under MFR, it would decrease by 1.5 million (−9%). In Europe, it would decrease by 109 000 (-4%) deaths under CLE, and 219 000 (-8%) under MFR. In France, the decrease would be of 7100 (−5%) deaths under CLE, and 11 700 (−8%) under MFR (Table 1). Corresponding concentrations can be found in Table S1 in the Supplementary material.

Table 1
Observed CV mortality in 2010 and expected number of CV deaths in 2030 and 2050 taken into account changes in $PM_{2.5}$ — Global, European and IdF scales.

Scale	World region	Annual CV mortality (number of deaths)[a]				
		2010 (baseline)	2030		2050	
			CLE (95% CI:)	MFR (95% CI:)	CLE (95% CI:)	MFR (95% CI:)
Global	World (192)	17243	17249 (17243, 17266)	15755 (16799, 14840)	17489 (17309, 17682)	15762 (16802, 14850)
	Europe (N = 38)	2775	2720 (2760, 2682)	2670 (2745, 2598)	2715 (2758, 2673)	2667 (2744, 2592)
	France	155	152 (154, 149)	149 (153, 146)	151 (154, 149)	149 (153, 145)
	IdF	17.7	–	–	17.2 (17.5, 16.8)	16.9 (17.4, 16.4)
	Paris	3.5	–	–	3.4 (3.5, 3.3)	3.4 (3.5, 3.3)
European	Europe (N = 38)	2775	2666 (2744, 2591)	2557 (2712, 2412)	2648 (2739, 2561)	2549 (2710, 2400)
	France	155	148 (153, 143)	143 (151, 135)	146 (152, 140)	142 (151, 134)
	IdF	17.7	–	–	16.2 (17.2, 15.2)	15.4 (17, 14)
	Paris	3.5	–	–	3.2 (3.4, 3)	3 (3.4, 2.7)
IdF	IdF	17.7	–	–	15.6 (17.1, 14.3)	14.8 (16.8, 13.1)
	Paris	3.5	–	–	3 (3.4, 2.7)	2.8 (3.3, 2.4)

All estimates are for population older than 15 years of age.
[a] *1000.

3.2.1. Global scale

1.5 [95% CI: 0.4, 2.4] million CV deaths could be delayed each year in 2030 compared to 2010 under MFR scenario (Fig. 2, Table S2). 84% of this benefit (nearly 1.3 million delayed deaths) would occur in Asia. The 0.82 million (nearly 55%) of these belong in China and 0.24 million (16%) in India.

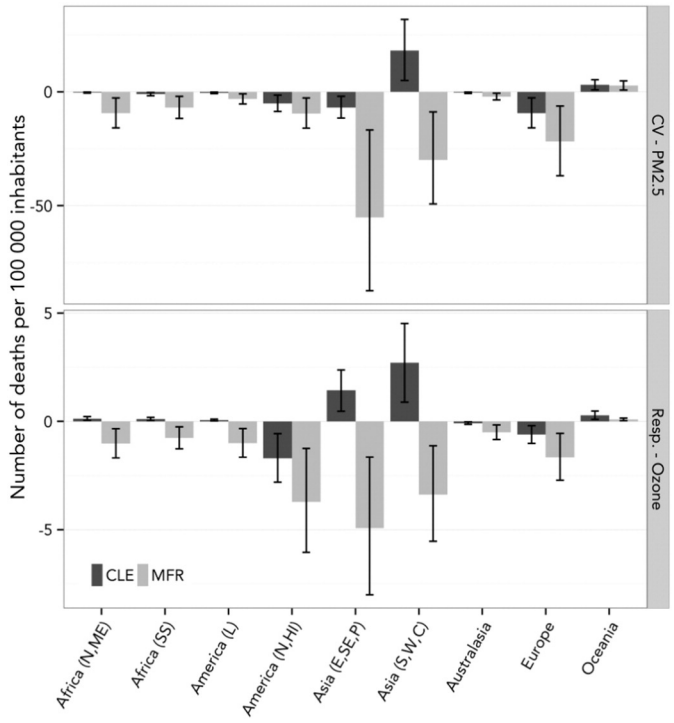

Fig. 2. Predicted changes in CV and respiratory mortality per 100 000 inhabitants associated with $PM_{2.5}$ and O_3, respectively, in 2030 under CLE and MFR scenarios including CRF limits (95% CI).

By contrast, under CLE scenario, additional CV deaths due to $PM_{2.5}$ would occur each year; nearly 7000 in 2030 and 0.25 million in 2050, compared to 2010. The largest increases in the number of CV deaths are projected in South Asia (85% of total Asia increases), the largest part of which belong in India (over 0.15 million).

In Europe, we expect decreases in CV mortality with both scenarios. Under MFR, nearly 0.14 (0.04, 0.23) million could be delayed in 2030 compared to 2010 (9% of total world reductions) (Fig. 2). The spatial repartition of impacts for 2030 is illustrated in Fig. S6 (Supplementary material).

3.2.2. Europe scale

In Europe, both scenarios concluded that air pollution-related mortality should decrease in 2030 compared to 2010 (Fig. S7); by nearly 8% for CV mortality, and 0.3% for respiratory mortality under MFR. The benefits under MFR scenario (219 000 CV deaths) are noticeably larger than those under CLE (109 000 CV deaths). Again, most of the changes should happen before 2030.

Under MFR, most benefits are expected in Central and Eastern Europe (especially Bulgaria, Belarus, Romania and Ukraine) for $PM_{2.5}$-related deaths and in Western Europe (especially Spain, Hungary and Italy) for O_3-related deaths under both, CLE and MFR scenarios (Table S3, Fig. 3). These estimated changes in CV and respiratory deaths are directly affected by the population-weighted contribution of the concentration levels in each country, that is why there is a considerable difference between Switzerland and Ukraine in $PM_{2.5}$-related deaths, for example.

3.2.3. Ile-de-France scale

The IdF pattern is consistent with the global and regional scale results: more reductions in deaths are expected under MFR, and the benefits associated with $PM_{2.5}$ changes largely exceed the benefits associated with ozone changes. More than 2830 annual CV deaths could be delayed in IdF in 2050 compared to 2010, with a distribution of benefits across towns (Table 2, Fig. 4). The larger reductions in CV mortality (14% under CLE and 20% under MFR compared to 2010) are expected in the city area of Paris, where $PM_{2.5}$ could decrease by more than 80% under the MFR scenario.

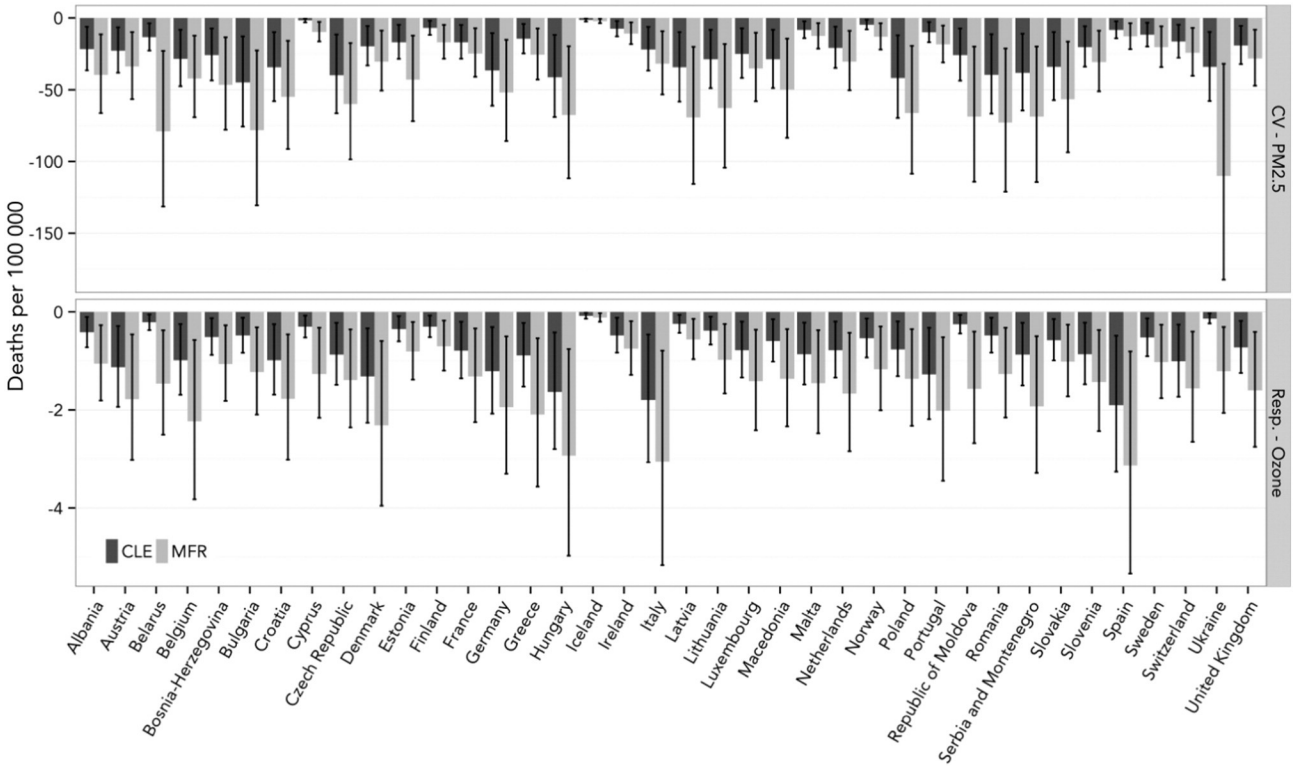

Fig. 3. Predicted changes in CV and respiratory mortality per 100 000 inhabitants associated with $PM_{2.5}$ and ozone in Europe in 2030 compared to 2010 under CLE and MFR scenarios (the error bars were computed with 95% confidence interval of the RR). Results are by country.

For O_3, we expect that the respiratory mortality will increase in the city of Paris by 0.6% under CLE and by 0.3% under MFR (relative to baseline) and decrease in rural areas (by 2.0% under CLE and by 2.7% under MFR) (Fig. 4).

3.3. Influence of the geographical scale: global vs. regional and regional vs. local

In this study the global and regional models use identical air pollutant emissions. The INCA global model has been recently improved to include chemistry of secondary inorganic aerosols, becoming closer to regional air quality models. The only major discrepancy in model formulation is the lack of secondary organic aerosol in the global model. In addition, model resolution may have a significant impact on HIA, as a finer scale allows a better assessment of population exposure.

For the same geographical domain area, the 2010 $PM_{2.5}$ concentrations modeled at the European scale were about twice as large as the global scale $PM_{2.5}$. The slope of the relationship between European and global scale was 1.69 ($r^2 = 0.76$) and remained almost unchanged in the future concentrations (Fig. 5, Fig. S8). This discrepancy in concentrations, which is caused mostly by the different models used, increased the discrepancy in CV mortality to 2.32 ($r^2 = 0.98$). This factor increased when we estimated the present burden of $PM_{2.5}$ on CV mortality using concentrations over 3 μg/m^3, to 4.64 ($r^2 = 0.86$), that is about 246 000 CV deaths at the European scale vs. 45 000 CV deaths at the global scale (Fig. 5). The 3 μg/m^3 threshold is the minimum concentration (that we could find) used in the cohort studies, from which Hoek et al. (2013) pooled the relative risks for cardiovascular mortality. The ratio between the 2010 $PM_{2.5}$ reduced to the threshold and total $PM_{2.5}$ concentrations was on average 1.5 for the European scale estimates and 4.2 for the global scale.

The discrepancy between global and European scales in $PM_{2.5}$ changes in 2030 or 2050 relative to 2010 under both scenarios was about 1.5; here, the discrepancy could also be affected by the difference

Table 2
Present population and annual CV mortality baseline, and future changes in cardiovascular and respiratory deaths associated with population-weighted annual $PM_{2.5}$ and ozone in 2050 compared to 2010 — Ile-de-France Scale.

IdF area	Number of communes	Pop., 2010	Annual CV mortality baseline, 2010	Future changes in CV deaths due to $PM_{2.5}$		Annual resp. mortality baseline	Future changes in resp. deaths due to O_3	
				2050-baseline			2050-baseline	
				CLE (95% CI)	MFR (95% CI)		CLE (95% CI)	MFR (95% CI)
Paris	20	1 913 400	3507	−496 (−147, −805)	−699 (−212, −1 108)	876	+5 (+1, +9)	+2 (+1, +4)
Paris Suburbs	411	6 482 500	11 802	−1 369 (−402, −2 242)	−1 883 (−563, −3 031)	2812	−26 (−7, −45)	−43 (−11, −74)
Rural areas	869	1 040 300	2353	−183 (−53, −305)	−253 (−74, −416)	576	−11 (−3,−19)	−15 (−4, −26)
IdF total	1300	9 436 100	17 662	−2 049 (−602, −3 351)	−2 835 (−849, −4 555)	4264	−33 (−8, −56)	−56 (−14, −96)

All estimates are for population older than 15 years of age; Pop. — population counts.

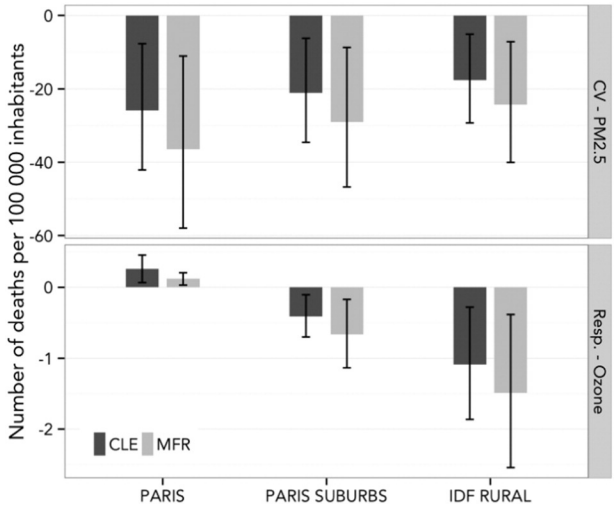

Fig. 4. Predicted changes in CV and respiratory mortality per 100 000 inhabitants associated with $PM_{2.5}$ and ozone in IdF in 2050 compared to 2010 under CLE and MFR scenarios (the error bars were computed with the 95% confidence interval of the RR).

in climate evolution used in the two models. Consequently, reductions in CV deaths projected with the global model are less than half of those obtained with the European scale (Table 3, Fig. S9).

For ozone, the global and European scale future estimates generally agree for almost all countries in Europe (Fig. S10, Supplementary material).

Assuming that this relationship can be extrapolated to other world regions, we estimated the underestimation of $PM_{2.5}$-related CV deaths derived from the global scale modeling. After applying the correction model, we computed that 329 300 additional $PM_{2.5}$-related CV deaths could occur in 2030 compared to 2010, which is 50 times larger than the initial global scale estimates. Benefits under MFR would increase by more than 1 million CV-related deaths (Table 4).

For IdF domain, the IdF scale $PM_{2.5}$ concentrations were larger than those derived from the European scale. A comparison between these two scales can be found in the Supplemental material (Fig. S11, Table S4). In that case the larger differences were obtained for ozone. Both scales mostly agree on their modeled concentrations in the IdF totals, because the results are dominated by the rural areas, which cover the majority of the IdF domain. When we separate the highly populated city of Paris from the rural areas, the results for Paris show larger discrepancy; increases in O_3 concentrations at the IdF scale and decreases at the European scale. Consequently, impacts of ozone changes on respiratory mortality over Paris were 15 times larger at the IdF scale rather than the European scale, under MFR. Indeed, the two scales used different scaling methodologies for emissions and due to the resolution constrains at the European scale the ozone chemistry inside the city cannot be captured with the same precision as it is at the IdF scale (see Section 3.1.3).

4. Discussion and conclusions

4.1. Main results

We used the same methodology on three different geographical scales to estimate the long-term future effects of $PM_{2.5}$ on cardiovascular mortality and O_3 on respiratory mortality. Keeping consistent methodology across the scales is a hard task, especially because of the lack of consistent datasets and emissions scenarios among scales. The interdisciplinary approach complements the understanding of processes from different points of view and provides shared access to various methods that can help achieve the common goal.

On every scale, large public health benefits are expected under MFR, while the burden of AP on mortality could worsen in many places under CLE. Yet, some countries, especially in Africa, would not benefit from an air quality improvement even under MFR.

In Europe, under MFR the CV deaths can be reduced by nearly 219 000 deaths and respiratory deaths by 109 000 deaths in 2030 relative to 2010. In 2050, in some regions, climate change would have a negative impact and counterbalance the benefits obtained in 2030 because of air pollution policies.

The large numbers obtained under MFR only quantify a small part of the overall health benefits associated with air pollution improvement, since we could not quantify the benefits on morbidity or on the prevalence of some chronic diseases for instance. MFR scenario is considered unrealistic because of its costs (Amann et al., TSAP report, 2013). However, public health benefits should also be taken into account and are clearly in favor of implementing the most ambitious scenario. It has to be noted that MFR only relies on technical solutions to reduce emissions. Other solutions can be adopted from the studies on behavior changes, such as promoting active transport in cities, which has been showed to generate large co-benefits through a general improvement in physical and mental health. Such strategies would reduce GHG emissions and therefore climate change. Although the long-term benefits of reducing the intensity of climate change cannot be quantified, they are believed to be huge; climate change is one of the greatest threats, which can affect health through multiple pathways (extreme events, modifications of the environment, infectious diseases, nutrition, risk of conflicts, etc.) (The Lancet Series, 2009).

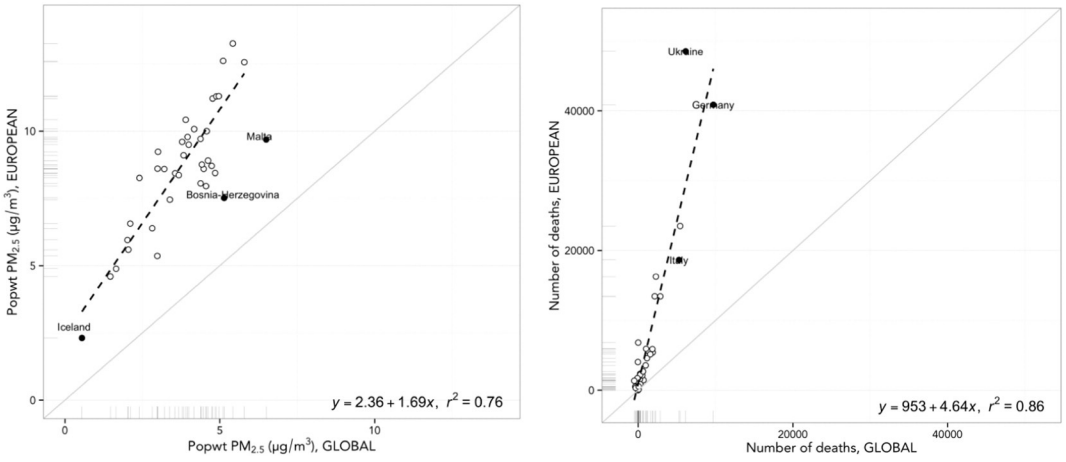

Fig. 5. Predicted population-weighted $PM_{2.5}$ concentrations (left) and CV mortality associated with $PM_{2.5}$ (right) in 2010: Comparison of the estimates obtained at the global and European scales for 38 countries in Europe. The red line indicates the linear fit between the global and European scale estimates. The solid points indicate the outliers according to Cook's distance.

Table 3
Predicted changes in population-weighted $PM_{2.5}$ concentrations and associated CV deaths in 2030 and 2050 compared to 2010 in Europe (N = 38 countries) at the global and European scales.

Health outcome	Year	Scenario	European countries at the global scale ($N_{countries}$ = 38)			European countries at the European scale ($N_{countries}$ = 38)		
			Conc. range, μg/m³	Avr. change in conc., μg/m³	Changes in CV deaths	Conc. range, μg/m³	Avr. change in conc., μg/m³	Changes in CV deaths
CV mortality due to $PM_{2.5}$	2030	CLE	0.5–5.7	−1.3	−55099	2.2–9.0	−2.4	−109398
		MFR	0.5–4.8	−2.6	−105356	2.0–7.5	−5	−218843
	2050	CLE	0.5–5.6	−1.4	−60538	1.9–8.4	−2.5	−127620
		MFR	0.5–4.6	−2.9	−108613	1.8–7.3	−5.1	−226523

All estimates are for population older than 15 years of age. The changes in CV mortality are relative to the present baseline mortality, which was 2775596 deaths annually.

4.2. Strength and limitations

This study used air pollution emissions scenarios (ECLIPSE), which are more suitable for air pollution studies than RCPs. Although RCPs include air pollutants, they were designed exclusively for the purpose of radiative forcing investigations as part of the Atmospheric Chemistry and Climate Model Intercomparison Project (ACCMIP) project (Shindell et al., 2012; Young et al., 2012). Their implementation for air quality projections constitutes a deviation of their primary purpose (Butler et al., 2012; Colette et al., 2012b; Fiore et al., 2012). Using scenarios designed for air quality provides a better quantitative view into the efficiency of air quality policies.

Regarding the robustness of the results, the global model (LMDz-INCA) has been extensively compared to measurements for both, ozone and particles (Hauglustaine et al., 2014; Folberth et al., 2006; Wang et al., 2014), and has been used in several model inter-comparison exercises (AEROCOM, ACCMIP, HTAP). All these exercises indicate that LMDz-INCA behaves properly and provides results in agreement with other state-of-the-art global models (the list of references can be provided). Similarly to the global model, the regional (CHIMERE) model has been extensively compared to other tools and observation (e.g., the Eurodelta, AQMEII, CityZen projects) (Bessagnet et al., 2014; Galmarini et al., 2012; Colette et al., 2011; Thunis et al., 2007). For the specific purpose of future projections, the present setup would benefit from using an ensemble approach (using several models for each scale). The goal of our project was to put together a single suite of models, but in the future uncertainties and robustness can only be addressed by using ensemble of models as a regular practice. On the local scale, the large uncertainties are associated with the implemented model resolution including that of the input emissions inventory, which is particularly important over urban areas.

We performed several sensitivity analyses on each scale and compared the influence of scale on results keeping other parameters constant. We found that HIA results for Europe derived from the global scale were nearly 50% lower than those based at the European scale model. This indicates that our global scale results may be largely under-estimated.

Indeed, regional scale models can account for a shorter-term variability of pollution in space and incorporate more complex chemical schemes than global models. They use inventories and trends designed

Table 4
Present population, annual CV mortality baseline and changes in CV mortality associated with population-weighted $PM_{2.5}$ in 2030 compared to 2010 — Comparison of the global scale estimates (base) and corrected global scale estimates (fitted).

World Region	Number of countries	Pop.,[a] 2010	Annual CV mortality baseline,[a] 2010	Changes in CV deaths[a], 2030 CLE-baseline		Changes in CV deaths[a], 2030 MFR-baseline	
				Base (95% CI)	Fitted (95% CI)	Base (95% CI)	Fitted (95% CI)
Africa (N,ME)	19	315899	926	−1.0 (−0.3, −1.8)	−5.5 (−1.6, −9.4)	−29.6 (−8.4, −50.1)	−64.0 (−18.4, −106.6)
Africa (SS)	46	469674	1295	−4.7 (−1.3, −8.0)	−6.7 (−1.9, −11.3)	−32.5 (−9.2, −55.1)	−65.1 (−18.7, −109.0)
America (L)	33	407461	989	−1.9 (−0.5, −3.2)	−9.9 (−2.8, −16.9)	−12.7 (−3.6,−21.6)	−35.2 (−10.0, −59.3)
America (N,HI)	2	275647	948	−13.9 (−3.9, −23.7)	−30.5 (−8.7, −51.6)	−26.0 (−7.4, −44.0)	−57.6 (−16.5, −96.3)
Asia (E,SE,P)	19	1668655	5568	−114.1 (−32.5, −192.3)	+27.6 (+7.4, +49.3)	−920.3 (−279.6, −1 458.9)	−1 459.0 (−467.1, −2 207.3)
Asia (S,W,C)	14	1101916	3393	+200.4 (+54.9, +351.1)	+476.5 (+126.3, +862.9)	−330.6 (−96.7, −543.1)	−565.4 (−170.4, −903.2)
Australasia	3	20400	60	−0.1 (−0.0, −0.1)	−0.7 (−0.2, −1.2)	−0.4 (−0.1, −0.7)	−1.7 (−0.5, −2.8)
Europe	43	623945	4050	−58.2 (−16.5, −98.8)	−121.6 (−34.6, −205.1)	−136.2 (−38.7, −230.0)	−286.9 (−82.7, −477.6)
Europe	38	498142	2775	−55.1 (−15.6, −93.5)	−108.9 (−31.0, −183.5)	−105.4 (−30.0, −177.6)	−215.7 (−62.3, −358.3)
Europe[b]	38	498142	2775	−109.4 (−31.2, −184.1)	–	−218.8 (−63.3, −363.1)	–
Oceania	13	5349	14	+0.2 (+0.0, +0.3)	+0.2 (+0.1, +0.4)	+0.1 (+0.0, +0.3)	+0.1 (+0.0, +0.2)
World[c]	192	4888946	17243	+6.6 (−0.1, +23.4)	+329.3 (+84.1, +617.1)	−1 488.3 (−443.7, −2 403.2)	−2 534.7 (−784.3, −3 962.0)

All estimates are for population older than 15 years of age. Pop. — population counts; N — north; ME — Middle East; SS — Sub-Saharan; L — Latin; HI — High Income; E — East; SE — South-East; P — Pacific; S — South; W — West; C — Central; the highlighted rows are not included in the world's total estimate.

[a] *1000.

[b] European scale estimates.

[c] The total do not include European estimates for 38 countries.

for such regional scales therefore they are more relevant for regional climate and air-quality policymaking. Also the results of regional modeling can often be compared across nearby countries. However, using relatively coarse horizontal resolutions (e.g., 50 km grid) in regional scale applications may be unsuitable when describing air pollution in urban agglomerations with high population density. It must be noted that while high model resolution can resolve transport and chemistry more efficiently, in order to describe city-scale trends, their emissions scenarios should also be developed by implementing a bottom-up approach utilizing activity information at such urban scale. In Markakis et al. (2014), where emission fluxes are taken from a local inventory to model air pollution in the area integrating only local scale data it was shown that the emission input can have a profound impact in modeled air quality compared to regional scale assessments implementing coarse inventories and resolutions.

Likewise, working at the IdF scale, the results were more than 20% larger than those estimated at the European scale for the same area of interest. Here the discrepancy can be mainly due to the resolution change. The differences were much smaller compared to the discrepancy between the European and global scales. This is partly because the same model was used at the European and IdF scales (CHIMERE). But it could also be because the gap in model resolution becomes less sensitive between the regional and local scales when focusing on the domain-wide totals, which represent the rural areas. We have shown that the change in resolution can have a profound effect when focusing on areas with large emission gradients such as cities (Markakis et al., 2014).

For ozone, the discrepancy between the scales is larger than for PM. The European scale reductions are larger than those at the IdF scale by more than 60%. Also, by increasing the resolution over the city area of Paris the future ozone concentrations and the related deaths at the IdF scale increased in contrast with the European scale where the concentration decreased. Consistently, Thompson and Selin (2012) performed uncertainty analysis using different resolutions (from 36 km to 2 km) and they found lower reductions in modeled ozone concentrations at a finer resolution (4–2 km) than it was at more coarse one (36 km) over several large U.S. cities.

Using future population and baseline mortality projections instead of keeping them constant reduced the benefits obtained with MFR scenario and enhanced the negative impact under CLE scenario for most of the world regions (Table S5). Using constant population and baseline mortality, in 2030 in Europe, under MFR scenario, the number of CV deaths could be reduced by 105400 (95% CI: −30000, −177600) deaths at the global scale and by 218800 (95% CI: −63300, −363100) deaths at the European scale. Taken into account changes in population and baseline mortality in the future, the CV deaths could be reduced by 185900 (95% CI: −53800, −308500) deaths under the MFR scenario at the European scale, 54% of which belong to females and 46% to males (Fig. 6).

Our choice of CRF might not be representative for all developing countries, but it is sufficient in our case; there were no robust long-term (cohort based) studies of $PM_{2.5}$-CV and ozone-respiratory RRs from those regions. Because the range of exposure to $PM_{2.5}$ from diverse sources can vary widely in time and space, the relation between $PM_{2.5}$ exposure and excess mortality RR is not necessary to be described as linear (Pope et al., 2009, 2011; Burnett et al., 2014). However, because we did not obtain $PM_{2.5}$ values higher than 55 μg/m^3 and the pattern of the non-linear relationship between CV mortality and $PM_{2.5}$ is not known (so it is between respiratory mortality and O_3), we used linear function instead of, for example, non-linear IER function (Burnett et al., 2014). Also, considering that only 5% of the world population is exposed to the values greater than 30 μg/m^3 the pattern of the relationship between CV mortality and $PM_{2.5}$ could be described as almost linear.

All studies to-date assume that the CRFs observed today will still be valid in the future. The assumption of constant baseline rates and constant CRFs does not take into account changes in the health-care system or in the vulnerability of the population, including aging, nor potential changes in the composition of future air-pollution mixtures. In the near future more CRFs should be available for more pollutants, including PM components, and new air-quality models will provide data for multiple PM components. Specifically, different components of PM may result in differing health impacts. With a careful methodology accounting for the possible interactions between the components, their effects on health can be better identified. And using multi-pollutant modeling approaches can provide useful uncertainty estimates.

4.3. Perspectives

HIAs exploring the joint effect of climate and air-pollution policies are of particular interest to policy-makers as they can illustrate the direct consequences of costly policies. An effort to communicate effectively with policy makers on the impacts of air quality emissions' policies and of mitigation policies on air pollutants and on greenhouse gases, and their joint impacts on health, is urgently needed.

The projection of future health impacts of air pollution may play an important role in policy discussions on air pollution and climate mitigation by illustrating the health effects of alternative air pollution scenarios and of mitigation policies, and the possible negative influence of climate change on air pollution. Consistent set of methods for carrying out such projections has not yet emerged and a challenge for future HIAs is to better understand and describe the uncertainties and public-health implications of the different choices made for the exposure modeling and scenarios.

HIAs provide results that may help decision-makers choose between different policy alternatives at different scales. Global scale studies include by design chemical mechanism that represents large-scale chemical interactions relevant for international climate policy. They provide comprehensive information across multiple continents and countries and are likely to be relevant in the context of global negotiations over greenhouse gas control policies. However, their capacity to represent local to regional air-quality policy is limited because of data quality control, data comparability across countries and scalability, and their HIAs are likely to be underestimated.

One important input for a policy decision is an explicit knowledge about the level of uncertainty of the information they get. The quantitative techniques used in the HIA analysis have the potential to provide the confidence levels ascribed to the results so that they can be taken into account by policy-makers in their own quantitative risk estimates. In this study we were able to propose a first view into the uncertainties arising from using multiple climate/air quality models, climate/emissions change scenarios, and multiple geographical scales.

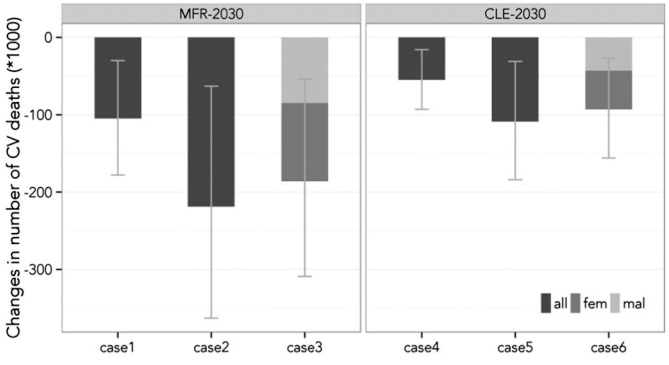

Fig. 6. CV mortality associated with $PM_{2.5}$ in Europe in 2030: Uncertainties due to the model choice (LMDz-INCA, CHIMERE), scenario (MFR, CLE), and the use of future baseline mortality and population including 95% CI. Cases 1 and 4: LMDz-INCA model, constant mortality baseline and population; Cases 2 and 5: CHIMERE model, constant mortality baseline and population; Cases 3 and 6: CHIMERE model, changed mortality baseline and population.

Acknowledgments

The study was done within the Air Pollution–Climate Change Health Impact Assessment (AC-HIA) project funded by the GIS-Climat, the French Environment and Energy Management Agency Ademe, contract n° 1110C0073. Z. Klimont was supported by the European Commission 7th Framework funded project ECLIPSE (Evaluating the Climate and Air Quality Impacts of Short-Lived Pollutants) Project no. 282688.

Appendix A. Supplementary data

Supplementary data to this article can be found online at http://dx.doi.org/10.1016/j.scitotenv.2015.02.002.

References

AIRPARIF, 2012. Evaluation prospective des émissions et des concentrations des polluants atmosphériques a l'horizon 2020 en Ile-De-France – Gain sur les émissions en 2015. Report available at http://www.airparif.asso.fr/_pdf/publications/ppa-rapport-121119.pdf.

Amann, M., Bertok, I., Borken-Kleefeld, J., Cofala, J., Heyes, C., Höglund-Isaksson, L., et al., 2011. Cost-effective control of air quality and greenhouse gases in Europe: modeling and policy applications. Environ. Model. Softw. 26, 1489–1501.

Amman, M., Klimont, Z., Wagner, F., 2013. Regional and global emissions of air pollutants: recent trends and future scenarios. Annu. Rev. Environ. Resour. 38, 31–55.

Anenberg, S.C., Schwartz, J., Shindell, D., Amann, M., Faluvegi, G., Klimont, Z., et al., 2012. Global air quality and health co-benefits of mitigating near-term climate change through methane and black carbon emission controls. Environ. Health Perspect. 120 (6), 831–839.

Amann, M., Bertok, I., Borken-Kleefeld, J., Cofala, J., Hettelingh, J.P., Heyes, C., et al., 2013. TSAP Report No 10. Policy Scenarios for the Revision of the Thematic Strategy on Air Pollution, Version 1.1 IIASA.

Balkanski, Y., 2011. L'Influence des Aérosols sur le Climat, Thèse d'Habilitation à Diriger des Recherches. Université de Versailles Saint-Quentin, Saint-Quentin-en-Yvelines.

Beelen, R., Raaschou-Nielsen, O., Stafoggia, M., Andersen, Z.J., Weinmayr, G., Hoffmann, B., et al., 2013. Effects of long-term exposure to air pollution on natural-cause mortality: an analysis of 22 European cohorts within the multicentre ESCAPE project. Lancet 383 (9919), 785–795. http://dx.doi.org/10.1016/S0140-6736(13)62158-3.

Bessagnet, B., Hodzic, A., Vautard, R., Beekmann, M., Cheinet, S., Honore, C., et al., 2004. Aerosol modeling with CHIMERE — preliminary evaluation at the continental scale. Atmos. Environ. 38, 2803–2817. http://dx.doi.org/10.1016/j.atmosenv.2004.02.034.

Bessagnet, B., Menut, L., Curci, G., Hodzic, A., Guillaume, B., Liousse, C., et al., 2008. Regional modeling of carbonaceous aerosols over Europe — focus on secondary organic aerosols. J. Atmos. Chem. 61, 175–202. http://dx.doi.org/10.1007/s10874-009-9129-2.

Bessagnet, B., Colette, A., Meleux, F., Rouïl, L., Ung, A., Favez, O., C., et al., 2014. The EURODELTA III exercise — model evaluation with observations issued from the 2009 EMEP intensive period and standard measurements in Feb/Mar 2009. In: EMEP (Ed.), *TFMM & MSC-W Technical Report* CLRTAP, Geneva.

Burnett, R.T., Pope III, C.A., Ezzati, M., Olives, C., Lim, S.S., Mehta, S., et al., 2014. An integrated risk function for estimating the global burden of disease attributable to ambient fine particulate matter exposure. Environ. Health Perspect 122, 397–403. http://dx.doi.org/10.1289/ehp.1307049.

Butler, T.M., Stock, Z.S., Russo, M.R., Denier van der Gon, H.A.C., Lawrence, M.G., 2012. Megacity ozone air quality under four alternative future scenarios. Atmos. Chem. Phys. 12, 4413–4428.

Center for International Earth Science Information Network (CIESIN)/Columbia University, Centro Internacional de Agricultura Tropical (CIAT), 2005. Gridded Population of the World, Version 3 (GPWv3): Population Density Grid. NASA Socioeconomic Data and Applications Center (SEDAC), Palisades, NY (http://sedac.ciesin.columbia.edu/data/set/gpw-v3-population-density (Accessed: 23 January 2013)).

Colette, A., Granier, C., Hodnebrog, O., Jakobs, H., Maurizio, A., Nyiri, A., et al., 2011. Air quality trends in Europe over the past decade: a first multi-model assessment. Atmos. Chem. Phys. 11, 11657–11678.

Colette, A., Granier, C., Hodnebrog, O., Jakobs, H., Maurizio, A., Nyiri, A., et al., 2012a. Future air quality in Europe: a multi-model assessment of projected exposure to ozone. Atmos. Chem. Phys. 12, 10613–10630.

Colette, A., Koelemeijer, R., Mellios, G., Schucht, S., Péré, J.-C., Kouridis, C., et al., 2012b. Co-benefits of climate and air pollution regulations. The Context of the European Commission Roadmap for Moving to a Low Carbon Economy in 2050. ETC/ACM - EEA, Copenhagen, p. 78.

Fiore, A.M., Naik, V., Spracklen, D.V., Steiner, A., Unger, N., Prather, M., et al., 2012. Global air quality and climate. Chem. Soc. Rev. 41, 6663–6683.

Folberth, G.A., Hauglustaine, D.A., Lathière, J., Brocheton, F., 2006. Interactive chemistry in the Laboratoire de Météorologie Dynamique general circulation model: model description and impact analysis of biogenic hydrocarbons on tropospheric chemistry. Atmos. Chem. Phys. 6, 2273–2319. http://dx.doi.org/10.5194/acp-6-2273-2006.

Galmarini, S., Rao, S.T., Steyn, D.G., 2012. Preface. Atmos. Environ. 53, 1–3.

Hauglustaine, D.A., Hourdin, F., Walters, S., Jourdain, L., Filiberti, M.-A., Larmarque, J.-F., Holland, E.A., 2004. Interactive chemistry in the Laboratoire de Météorologie Dynamique general circulation model: description and background tropospheric chemistry evaluation. J. Geophys. Res. 109, D04314.

Hauglustaine, D.A., Balkanski, Y., Schulz, M., 2014. A global model simulation of present and future nitrate aerosols and their direct radiative forcing of climate. Atmos. Chem. Phys. 14, 11031–11063. http://dx.doi.org/10.5194/acp-14-11031-2014.

Heal, M., Doherty, R., Heaviside, C., Vieno, M., Stevenson, D., Vardoulakis, S., 2012. Health effects of climate change in the UK 2012. Chapter 3, 55–82.

Hoek, G., Krishnan, R.M., Beelen, R., Peters, A., Ostro, B., Brunekreef, B., Kaufman, J.D., 2013. Long-term air pollution exposure and cardio-respiratory mortality: a review. Environ. Health 12 (1), 43.

Hourdin, F., Musat, I., Bony, S., Braconnot, P., Codron, F., Dufresne, J.-L., et al., 2006. The LMDZ4 general circulation model: climate performance and sensitivity to parametrized physics with emphasis on tropical convection. Clim. Dyn. 27, 787–813.

IARC, 2013. Outdoor air pollution a leading environmental cause of cancer deaths. International Agency for Research on Cancer — Press Release, Lyon.

Jacob, D.J., Winner, D.A., 2009. Effect of climate change on air quality. Atmos. Environ. 43, 51–63.

Jacob, D., Petersen, J., Eggert, B., Alias, A., Christensen, O., Bouwer, L., et al., 2013. EURO-CORDEX: new high-resolution climate change projections for European impact research. Reg. Environ. Chang. 1–16.

Jerrett, M., Burnett, R.T., Pope III, C.A., Ito, K., Thurston, G., Krewski, D., et al., 2009. Long-term ozone exposure and mortality. N. Engl. J. Med. 360 (11), 1085–1095.

Klimont, Z., Kupiainen, K., Heyes, C., Cofala, J., Rafaj, P., Höglund-Isaksson, L., et al., 2013. ECLIPSE V4a: Global Emission Data Set Developed With the GAINS Model for the Period 2005 to 2050 Key Features and Principal Data Sources.

Klimont, Z., Hoglund, L., Heyes, Ch., Rafaj, P., Schoepp, W., Cofala, J., Borken-Kleefeld, J., Purohit, P., Kupiainen, K., Winiwarter, W., Amann, M., Zhao, B., Wang, S.X., Bertok, I., Sander, R., 2015n. Global Scenarios of Air Pollutants and Methane: 1990–2050 (in preparation for ACPD).

Koffi, B., Szopa, S., Cozic, A., Hauglustaine, D., van Velthoven, P., 2010. Present and future impact of aircraft, road traffic and shipping emissions on global tropospheric ozone. Atmos. Chem. Phys. 10, 11681–11705. http://dx.doi.org/10.5194/acp-10-11681-2010.

Krewski, D., Jerrett, M., Burnett, R.T., Ma, R., Hughes, E., Shi, Y., et al., 2009. Extended follow-up and spatial analysis of the American Cancer Society study linking particulate air pollution and mortality. Res. Rep. Health Eff. Inst. (140), 5–114.

Lathière, J., Hauglustaine, D.A., Friend, A.D., De Noblet-Ducoudré, N., Viovy, N., Folberth, G.A., 2006. Impact of climate variability and land use changes on global biogenic volatile organic compound emissions. Atmos. Chem. Phys. 6, 2129–2146. http://dx.doi.org/10.5194/acp-6-2129-2006.

Lozano, R., Naghavi, M., Foreman, K., Lim, S., Shibuya, K., Aboyans, V., et al., 2012. Global and regional mortality from 235 causes of death for 20 age groups in 1990 and 2010: a systematic analysis for the Global Burden of Disease Study 2010. Lancet 380 (9859), 2095–2128.

Markakis, K., Valari, M., Colette, A., Sanchez, O., Perrussel, O., Honore, C., et al., 2014. Air-quality in the mid-21st century for the city of Paris under two climate scenarios; from regional to local scale. Atmos. Chem. Phys. Discuss. 14 (1), 1–1238.

Mathers, C.D., Loncar, D., 2006. Projections of Global Mortality and Burden of Disease from 2002 to 2030. PLoS Med. 3 (11), e442. http://dx.doi.org/10.1371/journal.pmed.0030442.

Medina, S., Ballester, F., Chanel, O., Declercq, C., Pascal, M., 2013. Quantifying the health impacts of outdoor air pollution: useful estimations for public health action. J. Epidemiol. Community Health 67 (6), 480–483.

Menut, L., Bessagnet, B., Khvorostyanov, D., Beekmann, M., Colette, A., Coll, I., et al., 2013. Regional atmospheric composition modeling with CHIMERE. Geosci. Model Dev. Discuss. 6, 203–329.

Orru, H., Andersson, C., Ebi, K.L., Langner, J., Astrom, C., Forsberg, B., 2013. Impact of climate change on ozone related mortality and morbidity in Europe. Eur. Respir. J. 41, 285–294.

Pope III, C.A., Dockery, D.W., 2006. Health effects of fine particulate air pollution: lines that connect. J. Air Waste Manag. Assoc. 56 (6), 709–742.

Pope III, C.A., Burnett, R.T., Thun, M.J., Calle, E.E., Krewski, D., Ito, K., Thurston, G.D., 2002. Lung cancer, cardiopulmonary mortality, and long-term exposure to fine particulate air pollution. JAMA 287 (9), 1132–1141.

Pope, C.A., Burnett, R.T., Krewski, D., Jerrett, M., Shi, Y., Calle, E.E., Thun, M.J., 2009. Cardiovascular mortality and exposure to airborne fine particulate matter and cigarette smoke: shape of the exposure–response relationship. Circulation 120 (11), 941–948.

Pope, C.A., Burnett, R.T., Turner, M.C., Cohen, A., Krewski, D., Jerrett, M., et al., 2011. Lung cancer and cardiovascular disease mortality associated with ambient air pollution and cigarette smoke: shape of the exposure–response relationships. Environ. Health Perspect. 119 (11), 1616–1621.

Post, E.S., Grambsch, A., Weaver, C., Morefield, P., Huang, J., Leung, L.-Y., et al., 2012. Variation in estimated ozone-related health impacts of climate change due to modeling choices and assumptions. Environ. Health Perspect. 120 (11), 1559–1564.

Raaschou-Nielsen, O., Andersen, Z.J., Beelen, R., Samoli, E., Stafoggia, M., Weinmayr, G., et al., 2013. Air pollution and lung cancer incidence in 17 European cohorts: prospective analyses from the European Study of Cohorts for Air Pollution Effects (ESCAPE). Lancet Oncol. 14 (9), 813–822.

Rao, S., Pachauri, S., Dentener, F., Kinney, P., Klimont, Z., Riahi, K., Schoepp, W., 2013. Better air for better health: forging synergies in policies for energy access, climate change and air pollution. Glob. Environ. Chang. 23 (5), 1122–1130.

Rouïl, L., Honore, C., Vautard, R., Beekmann, M., Bessagnet, B., Malherbe, L., et al., 2009. PREV'AIR an operational forecasting and mapping system for air quality in Europe. Bull. Am. Meteorol. Soc. 90, 73–83. http://dx.doi.org/10.1175/2008bams2390.1.

Schulz, M., 2007. Constraining Model Estimates of the Aerosol Radiative Forcing. (Thèse d'Habilitation à Diriger des Recherches, Université Pierre et Marie Curie, Paris VI).

Lancet Series, The, 2009. Health and, climate change. http://www.thelancet.com/series/health-and-climate-change.

Shindell, D.T., Lamarque, J.F., Schulz, M., Flanner, M., Jiao, C., Chin, M., et al., 2012. Radiative forcing in the ACCMIP historical and future climate simulations. Atmos. Chem. Phys. Discuss. 12, 21105–21210.

Skamarock, W.C., Klemp, J.B., Dudhia, J., Gill, D.O., Barker, D.M., Duda, M.G., et al., 2008. A Description of the Advanced Research WRF Version 3. NCAR.

Szopa, S., Balkanski, Y., Schulz, M., Bekki, S., Cugnet, D., Fortems-Cheiney, A., et al., 2012. Aerosol and ozone changes as forcing for climate evolution between 1850 and 2100. Clim. Dyn. 1–28.

Taylor, K.E., Stouffer, R.J., Meehl, G.A., 2012. An overview of CMIP5 and the experiment design. Bull. Am. Meteorol. Soc. 93, 485–498.

Thompson, T.M., Selin, N.E., 2012. Influence of air quality model resolution on uncertainty associated with health impacts. Atmos. Chem. Phys. 12, 9753–9762.

Thunis, P., Rouil, L., Cuvelier, C., Stern, R., Kerschbaumer, A., Bessagnet, B., et al., 2007. Analysis of model responses to emission-reduction scenarios within the City Delta project. Atmos. Environ. 41, 208–220.

van der Werf, G.R., Randerson, J.T., Giglio, L., Collatz, G.J., Mu, M., Kasibhatla, P.S., et al., 2010. Global fire emissions and the contribution of deforestation, savanna, forest, agricultural, and peat fires (1997–2009). Atmos. Chem. Phys. 10, 11707–11735. http://dx.doi.org/10.5194/acp-10-11707-2010.

van Loon, M., Vautard, R., Schaap, M., Bergström, R., Bessagnet, B., Brandt, J., et al., 2007. Evaluation of long-term ozone simulations from seven regional air quality models and their ensemble. Atmos. Environ. 41, 2083–2097.

Vautard, R., Honoré, C., Beekmann, M., Rouil, L., 2005. Simulation of ozone during the August 2003 heat wave and emission control scenarios. Atmos. Environ. 39, 2957–2967.

Vautard, R., Schaap, M., Bergström, R., Bessagnet, B., Brandt, J., Builtjes, P.J.H., et al., 2009. Skill and uncertainty of a regional air quality model ensemble. Atmos. Environ. 43, 4822–4832.

Wang, R., et al., 2014. Exposure to ambient black carbon derived from a unique inventory and high resolution model. Proc. Natl. Acad. Sci. U. S. A. 111, 2459–2463.

World Health Organisation, 2011. WHO Mortality Data Base Documentation. World Health Organisation Health Statistics and Health Information Systems (Accessed: 18 December 2012).

Young, P.J., Archibald, A.T., Bowman, K.W., Lamarque, J.F., Naik, V., Stevenson, D.S., et al., 2012. Pre-industrial to end 21st century projections of tropospheric ozone from the Atmospheric Chemistry and Climate Model Intercomparison Project (ACCMIP). Atmos. Chem. Phys. Discuss. 12, 21615–21677.

Zhang, Y., Bocquet, M., Mallet, V., Seigneur, C., Baklanov, A., 2012. Real-time air quality forecasting, part I: history, techniques, and current status. Atmos. Environ. 60, 632–655.